Trend Deviation Analysis for Automated Detection of Defects in GPR Data for Road Condition Surveys

Alena Uus[1], Panos Liatsis[2], Gregory Slabaugh[1], Athanasios Anagnostis[3], Sam Roberts[4], Stephen Twist[4]

[1] City University London, Northampton Square, EC1V 0HB London, UK
[2] The Petroleum Institute, PO Box 2533, Abu Dhabi, UAE
[3] Center for Research and Technology – Hellas, GR 57001 Thessaloniki, Greece
[4] Met Geo Environmental Ltd., LS10 1SW Leeds, UK
alena.uus.2@city.ac.uk

Abstract - **This paper presents a novel approach for automated detection of defects and structural changes in GPR data acquired in HMA (Hot Mix Asphalt) road surveys. Unlike the majority of existing approaches for road GPR data processing that are mainly used for extraction of layer profile information, the proposed method focuses on automated identification of significant deviations in subsurface structure and material properties. It is based on the detection of variations in intensity trends of longitudinal lines of interpolated B-scans that are characterized by deviations above a defined threshold. The outputs include mapped defects and deterioration areas together with the locations of detected changes in road structure design.**

Keywords – **Road structural condition monitoring; Non-destructive testing; GPR processing; Automated defect detection**

I. INTRODUCTION

Ground penetrating radar (GPR) is an efficient and well accepted non-destructive testing (NDT) tool in road condition surveys [2,3] for extraction and tracking of layer profile information required for structural condition inventory [4], identification of high void content areas or presence of moisture in subsurface layers [5,6], and detection of such defects as delaminations between layers or cracks [7-9]. It is also widely employed in concrete bridge deck inspection [10] for detection of rebar corrosion and delaminations.

Traditionally, 2D GPR data processing is based on detection of road layer interfaces and identification of changes and discontinuities related to variations in subsurface structure and material properties or the presence of defects and deterioration areas. Pre-processing methods generally include [11]: background removal, zero-offset correction, frequency and wavelet filtering. Next, various methods for layer interface detection and time-to-depth conversion are used for road layer thickness assessment [12-13], while diffraction hyperbola detection methods are generally employed for structure mapping and identification of defects in concrete bridges [14]. Other methods for GPR data processing include deconvolution [15], independent component analysis [16], power curve analysis [17], and neural networks [18].

The majority of GPR road data processing software focus on automated detection and extraction of layer thickness and relative permittivity estimation, rather than detection of local defects. Although the presence of some of the defects is reflected in the layer profile information, the analysis requires user input for mapping and interpretation. At the same time, early detection of deteriorations for planning of maintenance measures is essential for preservation of road structural condition. Due to the large amount of GPR data collected during road surveys, there is a clear need for an automated GPR datastream processing to detect and map subsurface defects and structural changes for further analysis by experts.

This paper describes a novel approach for processing and analysis of GPR data in HMA road surveys based on automated identification of significant trend deviations in subsurface structure and material properties independently of road layer construction design. The implemented method is part of the post-processing software solution of the RPB HealTec (Road Pavements & Bridge Deck Health Monitoring / Early Warning Using Advanced Inspection Technologies) NDT multisensor system for road condition surveys [1].

The proposed method is described in Section II, followed by the analysis of the results, a discussion of future research directions and conclusions in Sections III and IV, respectively.

II. PROPOSED METHOD AND RESULTS

A summary of the proposed method for automated GPR data processing is presented in Fig. 1. It includes B-scan pre-processing for enhancement of the subsurface structural features, followed by the detection of interface reflection and interpolation of A-scans. Next, detection of defects, deteriorations and road design changes is based on the extraction of longitudinal line trend derivatives and identification of the regions characterised by a critical "degree of deviation", considered to be an indicator of significant changes in either structural or material properties. This approach is acceptable in the specific task of GPR data analysis for HMA roads, since the layer structure of flexible road types is uniform and expected to be unchanging in the longitudinal direction unless there is a presence of defects. Next, the output in the form of mapped trend deviation "alert" regions can be used in a decision support software in

combination with the extracted layer profile information for maintenance planning [19].
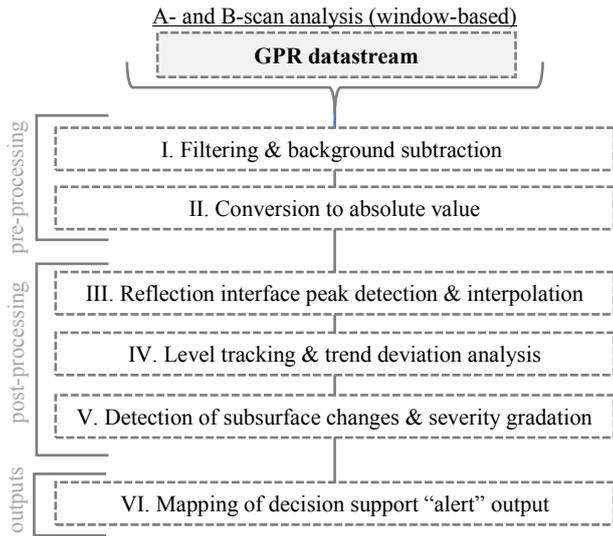

Figure 1.   GPR data processing: proposed method

The performance of the method was demonstrated on a GPR road scan segment, acquired during preliminary trials with an air-coupled 800 MHz MALA GPR antenna. The road segment consists of the HMA surface-binder, base and subbase layers and was reportedly free of surface defects. However, the GPR B-scan section shown in Fig. 2 indicates the presence of subsurface defects and structural changes. In the highlighted region, all layers are affected due to the presence of deteriorations in binder/base and base/subbase interfaces. There is a disturbance in the surface reflection with higher intensity corresponding to the material changes.
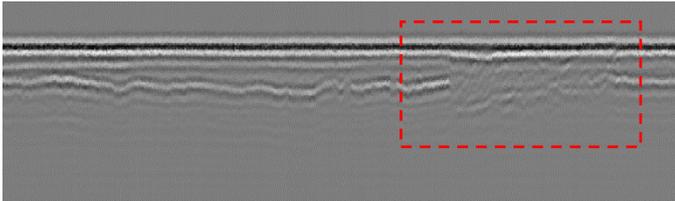

Figure 2.   GPR processing example: original B-scan with highlighted defects

GPR datastream processing is performed on a "window" basis with the B-scan window size (A-scans) set to a default value so that it fits within the specific display axes limits.

A.   Preprocessing of GPR data

Following median filtering for noise removal and background subtraction, the A-scans are converted to absolute value in order to perform analysis of positive and negative components of the original signal. Next, based on the detected reflection peaks, piecewise cubic interpolation is applied to every A-scan resulting in the continuous signal that comprises characteristics of interface reflections. Fig. 3 presents an example of a single A-scan pre-processing: (i) after filtering (A_F); (ii) after background subtraction and conversion to absolute value (A_{BG}); (iii) and interpolation (A_I).

The corresponding results for the investigated B-scan are shown in Fig. 4. It can be clearly seen how the layer structure within the deteriorated region is enhanced after the performed background subtraction and conversion to absolute value (Fig. 4.b). There is a significantly lower intensity of the reflection from the base-subbase layer interface caused by the change in the material properties as well as the structure deformation. The trend of the surface interface reflection is also affected with deviations in both structure and intensity.
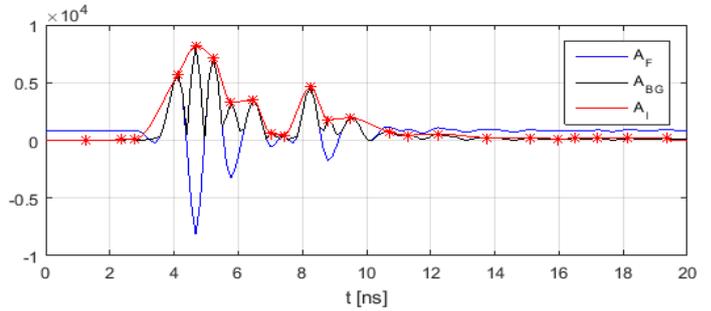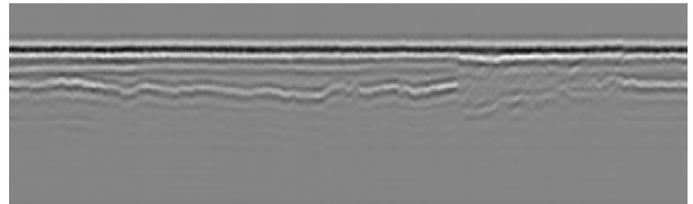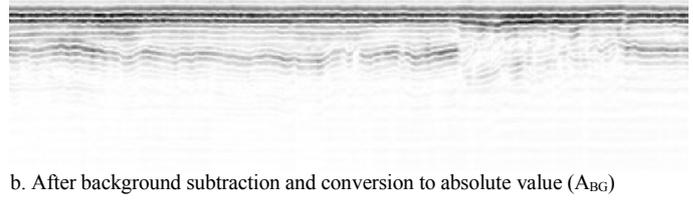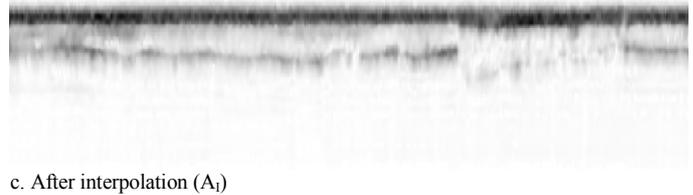

Figure 3.   GPR processing example: pre-processing stage (A-scan)

a. After filtering (A_F)

b. After background subtraction and conversion to absolute value (A_{BG})

c. After interpolation (A_I)

Figure 4.   GPR processing example: pre-processing stage (B-scan)

Peak-based interpolation (Fig. 4.c) provides the input for line-by-line trend analysis of the resulting B-scan. This approach has advantages in comparison to classical methods [11-13] that focus on the detected reflection peaks, which result in lower trend detection since the peak position and intensity magnitude can be disturbed due to various factors.

B.   Analysis of GPR data

Next, the interpolated B-scans are analysed for the presence of significant trend deviations in the layer profiles corresponding to either the presence of deteriorations or

changes in road construction design. The output is the mapping of the detected deviation locations with "alert" flags. The B-scan is automatically split into two regions corresponding to: (i) the HMA surface road layer and (ii) the base-subbase layers, Fig. 5. This procedure uses peak detection in the average A-scan. This "division" into regions does not affect the accuracy of defect detection and is mainly used in order to highlight and group defects with respect to their location and the number of regions can be increased.

Figure 5.   GPR processing example: division into layer regions

The deviations in the B-scan trends are tracked based on the analysis of the absolute derivative value of longitudinal line intensity levels. For instance, Fig. 6.b shows the intensity of the longitudinal lines of the top layer. Here, significant changes in the longitudinal level intensities can be observed in two regions (e.g., [75,125] and [325,375] A-scan sections).

a. Top layer of the interpolated B-scan

b. Longitudinal line trend intensities

c. Modulus of the trend derivatives with detected peaks above the threshold

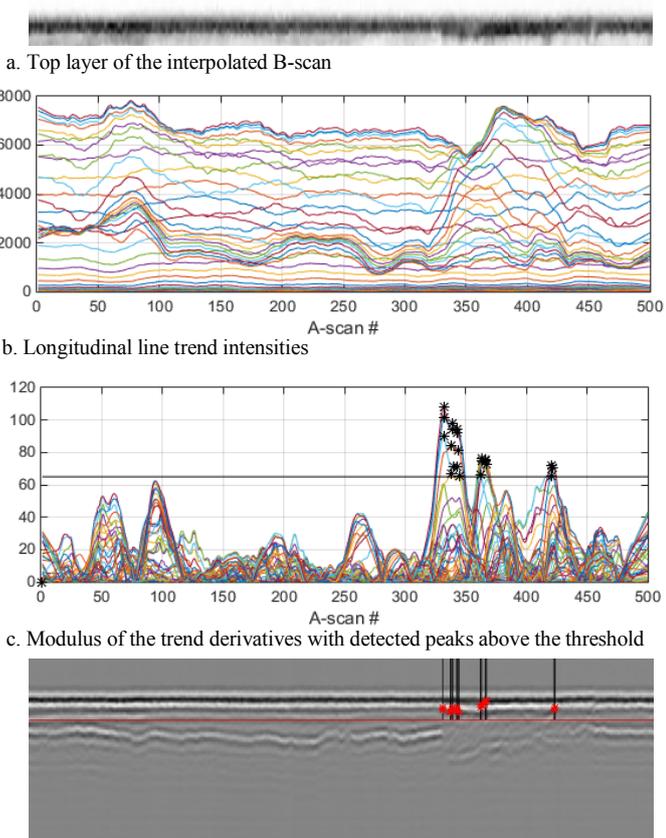d. Detected critical trend deviations mapped on the original B-scan

Figure 6.   GPR processing example: analysis stage (top layer)

Next, the modulus of the derivative of the longitudinal trend lines is determined, providing a characterization of trend

deviation. Significant defects or layer structure variations are detected using a threshold, set to a default value. In Fig. 6.c, the threshold is set to 65 and the absolute derivative values above this threshold are considered to be significant. Fig. 6.d shows the original B-scan with the deviation "alert" flags.

Post-processing results for the bottom layer region are shown in Fig. 7. All areas characterised by significant trend deviations (e.g., A-scan regions: [50,75], [300,350] and [425,475]) can be easily detected. Here, the mapped "alert" flags (Fig. 7.d) correspond to the changes of the base layer thickness and the presence of material deterioration.

a. Bottom layer of the interpolated B-scan

b. Longitudinal line trend intensities

c. Modulus of the trend derivatives with detected peaks above the threshold

d. Detected critical trend deviations mapped on the original B-scan
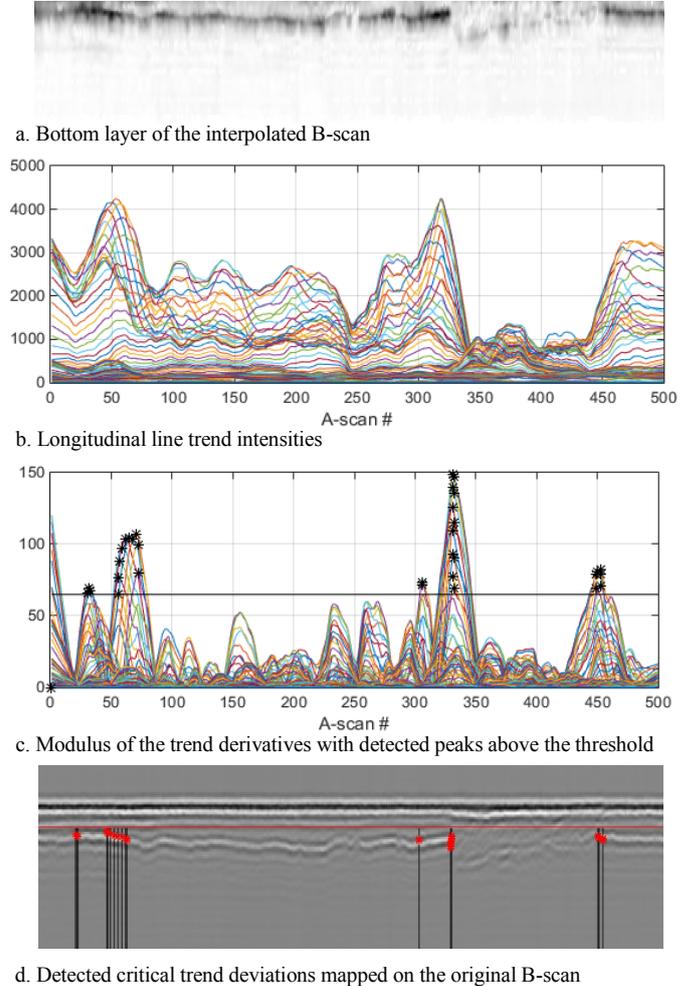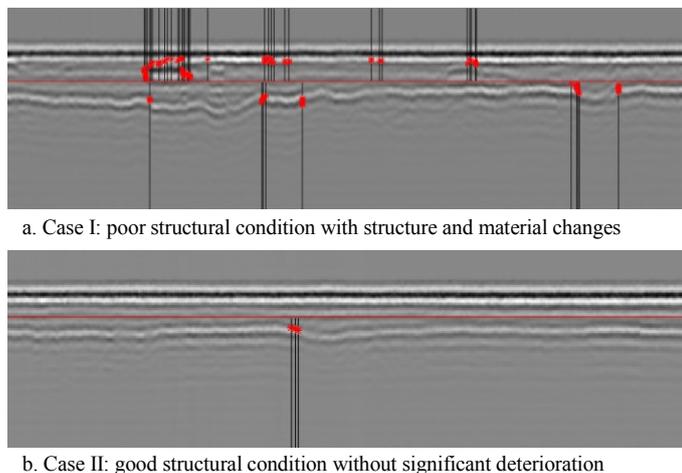
Figure 7.   GPR processing example: analysis stage (bottom layer)

III.   DISCUSSION AND FUTURE RESEARCH DIRECTIONS

The outputs of processing of GPR scans of two road segments with different degrees of deterioration are given in Fig. 8. In Case I, there is a clear presence of deviations in the layer interfaces and material property changes. The automated analysis successfully resulted in detecting delaminations in the HMA/base layer interface, areas of higher reflection intensity in the surface layer, and variations in the base layer structure profile. On the other hand, in Case II, only one significant deviation "alert" was mapped, which corresponds to the change in the base layer thickness.

a. Case I: poor structural condition with structure and material changes

b. Case II: good structural condition without significant deterioration

Figure 8.   Processing results for road segments with various deteriorations

It can be concluded that this method is effective in automated detection of subsurface changes and defects. However, defect detection sensitivity depends on the choice of the threshold. Therefore, this requires further optimisation to minimise false positive alarms. One of the proposed solutions is to use machine learning for automatic threshold adjustment. This necessitates analysis of the outcomes of the GPR field trials for various road designs and subsurface defect cases. Other parameters requiring investigation include the interpolation method and the degree of trend smoothing. The processing resulting can be further extended with the grading of defect severity based on the degree of trend change, analysis of reflection intensity value distribution and defect feature classification. The total number of "alerts" detected in one B-scan window can be used as a general characteristic of the road subsurface condition (or uniformity) and plotted along the entire length of the performed survey.

IV.   Conclusions

This paper presented a novel approach for automated analysis of GPR data in HMA road surveys for detection and mapping of the critical "changes" in structural and material properties of road layers. This can be used in road maintenance decision support systems in addition to the road layer profile characteristics extracted during routine GPR surveys.

One of the main advantages of the proposed solution is that it covers the entire range of possible subsurface changes rather than focusing on specific defect features as well as being independent of the HMA road structure type.

The effectiveness of this method together with the optimal approaches for the processing parameter adjustment will be investigated on future GPR field trials, since an extensive number of validated and annotated GPR data is required.

References

[1]   FP7 RPB HealTec project. [Online]. Available: www.fp7-rpbhealtec.org . [Accessed: 20 Jan 2016].

[2]   J. Hugenschmidt and P. Fürholz, "ATRAS – An automated GPR system for data acquisition and storage for roads and bridges," in 14th International Conference on Ground Penetrating Radar (GPR) June 4-8, 2012, Shanghai, China, 2012, pp. 448–453.

[3]   T. Saarenketo and T. Scullion, "Road evaluation with ground penetrating radar," J. Appl. Geophys., vol. 43, pp. 119–138, 2000.

[4]   I. L. Al-Qadi and S. Lahouar, "Measuring layer thicknesses with GPR – Theory to practice," Constr. Build. Mater., vol. 19, pp. 763–772, 2005.

[5]   J. Poikajärvi, K. Peisa, T. Herronen, P. O. Aursand, P. Maijala, and A. Narbro, "Nondestructive Testing and Evaluation GPR in road investigations – equipment tests and quality assurance of new asphalt pavement," Nondestruct. Test. Eval., vol. 27, no. 3, pp. 293–303, 2012.

[6]   D. Chen, F. Hong, W. Zhou, and P. Ying, "Estimating the hotmix asphalt air voids from ground penetrating radar," NDT E Int., vol. 68, pp. 120–127, 2014.

[7]   L. F. Walubita, T. Scullion, J. Leidy, and W. Liu, "Non-Destructive Testing Technologies: Application of the Ground Penetrating Radar (GPR) to Perpetual Pavements," Road Mater. Pavement Des., vol. 10, no. 2, pp. 259–286, 2009.

[8]   M. Celaya, "Evaluation of nondestructive technologies to assess presence and extent of delamination of hot mix asphalt airfield pavements," PhD Thesis, Univ. Texas El Paso, 2011.

[9]   L. Krysi and J. Sudyka, "GPR abilities in investigation of the pavement transversal cracks," J. Appl. Geophys., vol. 97, pp. 27–36, 2013.

[10] A. M. Alani, M. Aboutalebi, and G. Kilic, "Applications of ground penetrating radar (GPR) in bridge deck monitoring and assessment," J. Appl. Geophys., vol. 97, pp. 45–54, Oct. 2013.

[11] Sandmeier geophysical research, ReflexW Manual. [Online]. Available: www.sandmeier-geo.de/Download/reflexw_manual_a4_booklet.pdf . [Accessed: 20 Jan 2016].

[12] M. Solla, X. Nunez-Nieto, M. Varela-Gonzalez, J. MartInez-Sanchez, and P. Arias, "GPR for Road Inspection : Georeferencing and Efficient Approach to Data Processing and Visualization," in 15th International Conference on Ground Penetrating Radar - GPR, June 30 - July 4, 2014, Brussels, Belgium, 2014, pp. 913–918.

[13] S. Lahouar and I. L. Al-Qadi, "Automatic detection of multiple pavement layers from GPR data," NDT E Int., vol. 41, no. 2, pp. 69–81, 2008.

[14] Z. W. Wang, M. Zhou, G. Slabaugh, and T. Fang, "Automatic Detection of Bridge Deck Condition From Ground Penetrating Radar Images," IEEE Trans. Autom. Sci. Eng., vol. 8, no. 3, pp. 633–640, 2011.

[15] I. Abdel-Qader, V. Krause, F. Abu-Amara, O. Abudayyeh, "Comparative Study of Deconvolution Algorithms for GPR Bridge Deck Imaging," WSEAS Transactions on Signal Processing, vol. 10, pp. 20–31, 2014.

[16] F. Abu-amara, "An Automated Framework for Defect Detection in Concrete Bridge Decks Using Fractals and Independent Component Analysis," PhD Thesis, Western Michigan University, 2010.

[17] S. Colagrande, D. Ranalli, and M. Tallini, "Ground Penetrating Radar Assessment of Flexible Road Pavement Degradation," International Journal of Geophysics, vol. 11, 2011.

[18] Y. Cao, B. B. Guzina, and J. F. Labuz, "Pavement Evaluation Using Ground Penetrating Radar,." 1. Report No. MN/RC 2008-10, Minnesota Department of Transportation, 2008.

[19] S. Miah, A. Uus, P. Liatsis, S. Roberts, S. Twist, M. Hovens, H. Godding, and G. Nardoni, "NDT Sensor Fusion: Optimisation of NDT Sensor Data Processing Strategies for Road Infrastructure Inspection," in Universities' Transport Study Group (UTSG) Conference, January 6-8 2016, Bristol, UK, 2016.